Batteries & Supercaps

Research Article
doi.org/10.1002/batt.202400007

Chemistry Europe
European Chemical Societies Publishing

www.batteries-supercaps.org

Amino–Functionalized Multi–walled Carbon Nanotube/SPEEK Hybrid Proton Exchange Membrane for Iron–chromium Redox Flow Battery**

Enrui Bai+,[a, b] Chuanyu Sun+,[c] Haotian Zhu,[a, b] Zhihai Liu,[d] Chongyang Xu,*[a] Xiaoyin Xie,*[b, e] and Sheng Wu*[a]

In the field of iron–chromium redox flow battery (ICRFB), the optimal doping ratio of the amino–functionalized multi–walled carbon nanotube (MWCNT–NH_2) blended with SPEEK as hybrid proton exchange membrane (PEM) is determined to be 2 wt% by series tests. The ICRFB single–cell containing the S/MWCNT–NH_2–2 PEM was tested and compared with the Nafion 212 and original SPEEK PEMs. It is worth noting that the single–cell containing S/MWCNT–NH_2–2 exhibits significantly higher coulombic efficiency (CE: 96.06%) and energy efficiency (EE: 88.68%) under 40 mA cm^{-2} than that of the Nafion 212 (EE: 82.83%, CE: 88.9%). Differing from the original SPEEK PEM, it also exhibits higher EE (82.04%) than the Nafion 212 (81.09%) at 100 mA cm^{-2}. During the self–discharge test, the lower permeability of iron/chromium ions through S/MWCNT–NH_2–2 PEM also allows for a longer self–discharge time than the other two single–cells. Additionally, the single–cell containing S/MWCNT–NH_2–2 showed a smaller decay range of EE (from 82.67% to 77.36%) and more discharge capacity retention (48%) than that of the Nafion 212 (EE: from 82.64% to 75.01%, discharge capacity retention: 18%) after 100 cycles, which suggests that the hybrid SPEEK PEM with optimal content of MWCNT–NH_2 has a great potential to replace Nafion PEMs in the large-scale commercialization of ICRFB.

Introduction

Iron–chromium redox flow battery (ICRFB) is an important large–scale energy storage system, which has the advantage of economical electrolyte materials, environmentally friendly, safe, reliable, and long operating life.[1] Recently, it has regained the focus of attention due to the optimization of electrolytes and the suppression of hydrogen evolution problems.[2] During charging or discharging, Fe^{2+}/Fe^{3+} and Cr^{3+}/Cr^{2+} from anolyte/catholyte perform the redox reactions, which realize the mutual conversion between electrical energy and chemical energy of the whole system. Throughout the reaction process, the protons (H^+) form a closed conductive loop through the proton exchange membrane (PEM),[3] while the larger radius of Fe^{2+}/Fe^{3+} and Cr^{3+}/Cr^{2+} are blocked by the PEM on both sides. The specific electrochemical reaction equations of the ICRFB containing the mixed iron-chromium electrolyte are as follows.[4]

$$\text{Anode}: Fe^{2+} + Cr^{3+} \underset{\text{discharge}}{\overset{\text{charge}}{\leftrightarrow}} Fe^{3+} + Cr^{3+} + e^- \tag{1}$$

$$\text{Cathode}: Cr^{3+} + e^- + Fe^{2+} \underset{\text{discharge}}{\overset{\text{charge}}{\leftrightarrow}} Cr^{2+} + Fe^{2+} \tag{2}$$

$$\text{Cathode}: Cr^{3+} + e^- + Fe^{2+} \underset{\text{discharge}}{\overset{\text{charge}}{\leftrightarrow}} Cr^{2+} + Fe^{2+} \tag{3}$$

However, as the main subassembly of the ICRFB, the most widely used PEM is still dominated by the Nafion PEM. These commercial PEMs have the disadvantages of high price and low ion selectivity,[5] which impede the further industrial development of ICRFB.The sulfonated poly (ether ether ketone) (SPEEK) PEM is considered a strong competitor to the Nafion PEM due to its superiority of low budget, ease of preparation, and high ion selectivity.[6] However, it has a smaller degree of hydrophilic/hydrophobic phase separation and forms hydrophilic channels with smaller diameters accompanied by many bifurcations and end closures, which results in a weaker ability of proton transport than that of the Nafion PEM.[7] To improve the performance of the SPEEK PEM, researchers mainly adopt the methods of organic–inorganic materials doping. The common inorganic fillers include TiO_2,[8,9] WO_3,[10] KOH,[11]

[a] E. Bai,+ H. Zhu, C. Xu, S. Wu
Yantai Research Institute, Harbin Engineering University, Yantai Shandong 264003, China,
E-mail: xcy110@126.com
wusheng@hrbeu.edu.cn

[b] E. Bai,+ H. Zhu, Prof. X. Xie
School of Chemistry and Chemical Technology, Hubei Polytechnic University, Huangshi 435003, China,
E-mail: xyxie@hbpu.edu.cn

[c] C. Sun+
School of Electrical Engineering and Automation, Harbin Institute of Technology, Harbin 150006, China

[d] Z. Liu
School of Physics and Electronic Information, Yantai University, Yantai 264005, China

[e] Prof. X. Xie
Hubei Zhenhua Chemical Co. Ltd, Huangshi 435000, China

[+] These authors contributed equally

[**] SPEEK = Sulfonated poly (ether ether ketone)

Supporting information for this article is available on the WWW under https://doi.org/10.1002/batt.202400007 functionalized carbon black (FCB),[12] graphene oxide (GO)[13,14] and so on. Interface interactions such as hydrogen bonds, acid–base interactions, or ionic bonds between inorganic fillers and SPEEK polymer can effectively reduce the swelling rate of the hybrid PEM, and these interactions can also adjust the size of the proton transport channel, which is conducive to proton transport and effectively block the permeation of metal ions. In addition, inorganic fillers usually have the advantages of high mechanical strength and corrosion resistance, which help to improve the mechanical properties and chemical stability of the hybrid PEM.[15] Besides, The combination of SPEEK polymer with organic materials such as lignin[16,17] and SMA-SN[18] is also an effective method. By adjusting the composition of the membrane materials, the separation structure of the hydrophilic/hydrophobic phase can be controlled, so as to improve the water uptake, proton conductivity, ion selectivity, and other important properties of the SPEEK PEM. At present, there is a rare modification study of the SPEEK PEM applied for the ICRFB, which needs to be brought to the researchers' attention.

In our previous work, the SPEEK PEMs with five different degrees of sulfonation (DSs: 43%, 47%, 52%, 57%, and 62%) have been investigated in detail.[19] It can be concluded that the SPEEK PEM with DS = 57% exhibited the most balanced physicochemical properties. By further optimizing its thickness, the SPEEK 57–25 was prepared (DS: 57%, thickness: 25 μm). In the ICRFB single–cell tests, the single–cell containing SPEEK 57–25 performed higher EE than the Nafion 212 under 40–80 $mA\,cm^{-2}$. However, the EE of single–cell containing SPEEK 57–25 appeared to be lower than that of the Nafion 212 once exceeded 100 $mA\,cm^{-2}$ due to its higher inner resistance,[20] which means the original SPEEK 57–25 PEM should be modified by some high proton–conductive materials to obtain a broader application prospect. Multi–walled carbon nanotube (MWCNT) is widely used as an excellent filler material in the research of PEM modification, and its special structure can enhance proton transport efficiency. Moreover, the long and complex structure can also play a role in blocking the penetration of metal ions through the PEM. Besides, the great mechanical properties of MWCNT can also enhance the tensile strength of the hybrid PEM.[21]

In this study, the amino–functionalized MWCNT ($MWCNT-NH_2$) was employed to modify the SPEEK PEM. The acid–base interactions between sulfonic acid/amine groups can not only provide more channels for proton transport but also block the penetration of metal ions.[22] To determine the best content of the $MWCNT-NH_2$ powder, the physicochemical characteristics of ion exchange capacity (IEC), proton conductivity, water uptake (WU), swelling ratio (SR), permeability of iron ions and chromium ions, and mechanical properties were measured. Moreover, the ICRFB single–cell containing the optimal hybrid SPEEK PEM was tested to compare with the original SPEEK and Nafion 212 PEMs, and the results suggest that this optimal hybrid PEM has an enormous potential to be the substitute for the Nafion PEM in the ICRFB systems.

Experimental Section

Materials

Poly (ether ether ketone) (PEEK 450PF) was purchased from Victrex. Nafion 212 PEM was purchased from Chemours. $MWCNT-NH_2$ (length: 8–15 μm, inner diameter: 3–5 nm, external diameter: 8–15 nm, specific resistance: 1800 μΩ/m, specific surface area: ≥210 m^2/g) was provided by Shenzhen Tanxi Technology Co., Ltd. The other chemicals including H_2SO_4, NaOH, HCl, $FeCl_2\cdot 4H_2O$, $CrCl_3\cdot 6H_2O$, $AlCl_3\cdot 6H_2O$ and $MnCl_2\cdot 4H_2O$ were purchased from Sinopharm. The ICRFB single–cell components, such as graphite felt electrodes, graphite bipolar plates, and copper foils, were purchased from Wuhan Chuxin Technology Co., Ltd.

Preparation of SPEEK Polymer

To acquire the homogeneous SPEEK solution, the PEEK was sulfonated with H_2SO_4 (98%) in a 60 °C water bath for 5 h. With the mechanical stirring, the mixture was gradually dropped into the ice–cold water bath. The obtained white SPEEK fibers were rinsed until pH neutralized with plenty of deionized water, and the fibers were dried at 80 °C for 12 h in the drying furnace.[23]

Preparation of S/$MWCNT-NH_2$ Hybrid PEMs

0.3 g SPEEK fibers were dissolved into 10 mL N, N'-dimethylformamide (DMF), and the mixture was stirred in the water bath at 50 °C until the fibers were entirely dissolved. A specific mass of $MWCNT-NH_2$ powder was introduced to the SPEEK solution and dispersed using an ultrasonic disperser for 1 h after stirring thoroughly for 2 h to obtain a homogeneous solution. The mixture was delivered to a culture dish (diameter:10 cm), heated at 70 °C for 7 h and 90 °C for 3 h in a drying furnace. The culture dish was soaked in the deionized water to remove the PEM after it had cooled to the ambient temperature. Then the prepared PEM was immersed in 1 M sulfuric acid for 1 day to remove the impurities, and washed to neutral with lots of deionized water. At last, the PEM was stored in the deionized water at room temperature before tests. Figure 1 demonstrates the preparation procedures of the SPEEK/$MWCNT-NH_2$ hybrid PEM (S/$MWCNT-NH_2$ for short).

Characterizations

Morphology

The energy dispersive X-ray spectroscopy (EDX) element mapping images and surface morphology of the PEM were measured by scanning electron microscopy (SEM, JSM-7610F). The three–dimensional morphology of the PEM was captured by Atomic Force Microscopy (AFM, Dimension Fastscan).

IEC, WU, and SR

The obtained PEM was shaped into small pieces and immersed in the 50 mL saturated sodium chloride solution with mechanical stirring for 24 h. 0.01 M NaOH was used to determine the acidity of the above mixture. The IEC is based on the following equation:

$$IEC = \frac{V_{NaOH} \times C_{NaOH}}{W_{dry}} \quad (4)$$

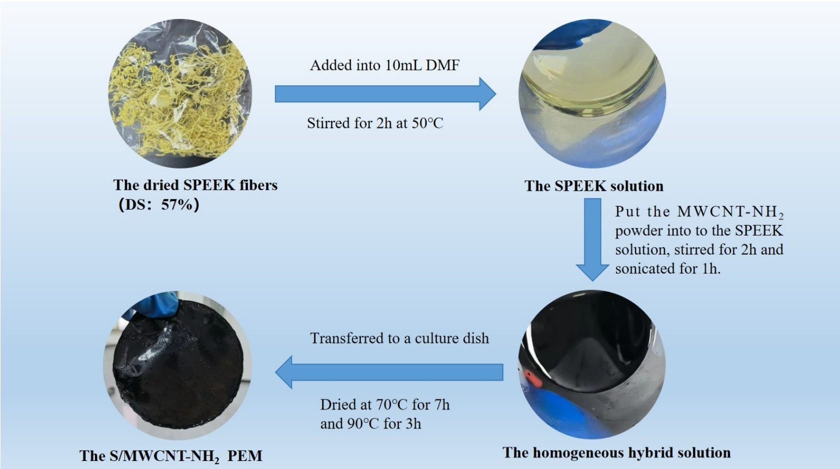

Figure 1. The preparation procedures of the SPEEK and MWCNT–NH$_2$ hybrid PEMs.

where V_{NaOH} and C_{NaOH} are the consumed volume and concentration of NaOH solution, and W_{dry} is the mass of the dried PEM.

To measure wet weight and length, the PEM was soaked in the deionized water at 65 °C for 12 h, and the surface water was wiped off immediately. To acquire the dry weight and length, the PEM was placed in the drying furnace at 90 °C for 12 h, and the data was measured rapidly once it contacted the air. The SR and WU are based on the following equations:

$$WU(\%) = \frac{Wwet - Wdry}{Wdry} \times 100\% \tag{5}$$

$$SR(\%) = \frac{Lwet - Ldry}{Ldry} \times 100\% \tag{6}$$

where L_{wet} and L_{dry} are the lengths of wet and dried PEMs, and W_{wet} and W_{dry} are the masses of wet and dried PEMs.

Proton Conductivity and Cr^{3+}/Fe^{2+} Permeability

The PEM was shaped into a square with a side length of 2 cm and immersed in the deionized water all day at 65 °C, then it was fastened to a fixture with two Pt electrodes, and this fixture was soaked in the deionized water at 65 °C. The internal resistance of the PEM was measured by the PGSTAT 302N electrochemical station through the function of electrochemical impedance spectroscopy (EIS). The conductivity is based on the following equation:[24]

$$\sigma = \frac{l}{w \times t \times r} \tag{7}$$

where w, t, and r are the width, thickness, and resistance of the PEM, and l is the length between the two Pt electrodes.

An H-type electrolytic reservoir was employed to test the permeability of Cr^{3+}, in which the left side consisted of 25 mL 3 M HCl + 1 M $CrCl_3$, and the right side consisted of 25 mL 3 M HCl + 1 M $AlCl_3$. The $AlCl_3$ solution plays the role of minimizing the osmotic pressure effect and equalizing the ionic strength. The prepared PEM was fixed in the middle of the two electrolytic reservoirs. Both reservoirs were mechanically agitated at 65 °C through the oil bath. At specific intervals, 3 mL solution from the right side reservoir was extracted to determine the Cr^{3+} permeability with the SPECORD S600 UV-vis spectrometer, and the solution was poured back into the reservoir after measuring. The test method of the permeability for Fe^{2+} ions was attached in the SI. The Cr^{3+}/Fe^{2+} permeability is based on the following equation:

$$VR\frac{dcR(t)}{dt} = A\frac{P}{l}[cL - cR(t)] \tag{8}$$

where $C_R(t)$ and C_L are Fe^{2+}/Cr^{3+} concentrations of the right and left solutions. P is the Fe^{2+}/Cr^{3+} permeability, A and l are the area and thickness of the PEM, and V_R is the volume of the right-side solution.

Mechanical Properties

The dried PEM was shaped into a 1 cm×5 cm rectangle and its mechanical properties was measured by the DR-509A universal testing machine. The stretch speed of the machine was 50 mm min^{-1}.

ICRFB Single–Cells Performance

Firstly, the graphite felt electrodes were pretreated, rinsed repeatedly with deionized water to remove inorganic impurities, then soaked in ethanol solution for 30 minutes to remove organic impurities, and finally dried in an 80 °C vacuum oven for 4 h to remove excess water. The size of the graphite felt electrodes is 0.3 cm×5 cm×5 cm (thickness, width and length). Besides, the other components were also rinsed with deionized water and wiped dry. The Nafion 212 membrane was immersed in 1 M sulfuric acid for 1 day to remove the impurities, and washed to neutral with lots of deionized water, then it was immersed in the deionized water at room temperature for 24 h to control the same state as the SPEEK membranes. Afterwards, the assembly of the ICRFB single–cell began. The PEM with a 5 cm×5 cm effective coverage was sandwiched between two graphite felt electrodes. Graphite bipolar plates and two copper foils are utilized as the current collectors. The catholyte and anolyte are both made up of 40 mL 3 M HCl + 1 M $CrCl_3$ + 1 M $FeCl_2$ mixed solution.[25] The ICRFB single–cell stack was placed in a 65 °C constant temperature furnace to keep the best operating environment.[26] Two DIPump550 peristaltic pumps were used to transfer the electrolytes, and the speed was set to 100 rpm.

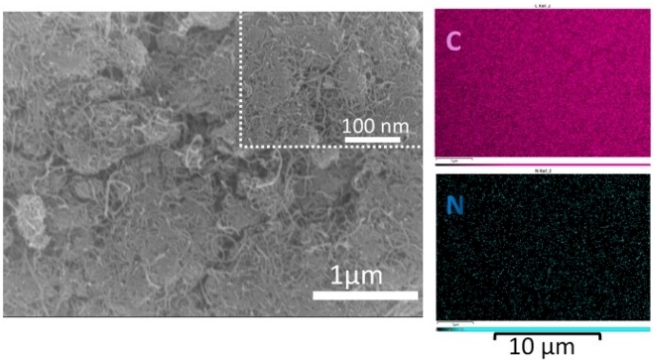

Figure 2. SEM and EDX of the MWCNT–NH_2 powder.

The electrochemical performance of the single–cell can be reflected by the stack resistance. To acquire this value, the ICRFB single–cell was operated without power for minutes and the stable resistance was measured by an RC3563 battery tester.

The CT3002K battery test system was employed to operate the tests of the single–cells containing different PEMs. The range of current density of the tests is 40–100 mA cm^{-2} with a 20 mA cm^{-2} interval. The 100-cycle tests were operated under 100 mA cm^{-2} to explore the long–term stability of the PEMs under the high current density. To conduct the self–discharge tests, the single-cells were uniformly charged to the state of charge (SOC) ≈ 50 % under 100 mA cm^{-2} and the cells were kept running without power.[27] Besides, the upper limit and the lower limit of the potential is 0.8 V and 1.2 V at the whole tests.[28] The coulombic efficiency (CE), energy efficiency (EE), and voltage efficiency (VE) are obtained based on the following equations:[29]

$$CE = \frac{\int Iddt}{\int Icdt} \times 100\% \quad (9)$$

$$EE = \frac{\int VdIddt}{\int VcIcdt} \times 100\% \quad (10)$$

$$VE = \frac{EE}{CE} \times 100\% \quad (11)$$

where V_c and V_d are the charge/discharge potentials. I_c and I_d are the charge/discharge currents.

Results and Discussion

SEM, EDX, and AFM

Figure 2 shows the SEM and EDX element images of MWCNT–NH_2 powders. The EDX of the nitrogen element in Figure 2 demonstrates that the amino groups are distributed uniformly in the MWCNT. Figure 3b shows the smooth surface of the S/MWCNT–NH_2–2 PEM. Compared with the original SPEEK PEM in Figure 3a, this hybrid PEM exhibits no obvious defects, which proves that the incorporation of MWCNT–NH_2 particles with SPEEK was successful.[30] Figures 4a and 4b show

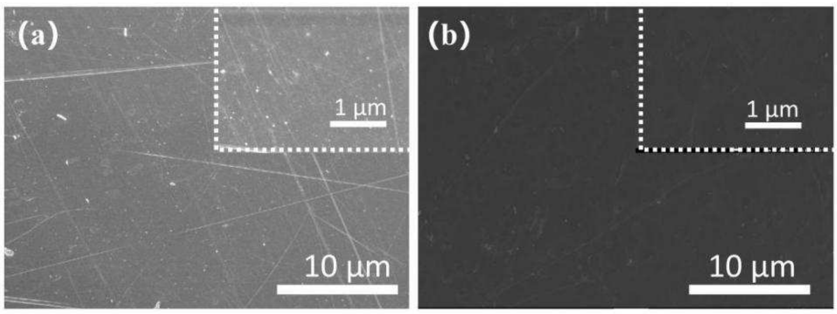

Figure 3. The surface SEM images of (a) the original SPEEK and (b) the S/MWCNT–NH_2–2 PEMs.

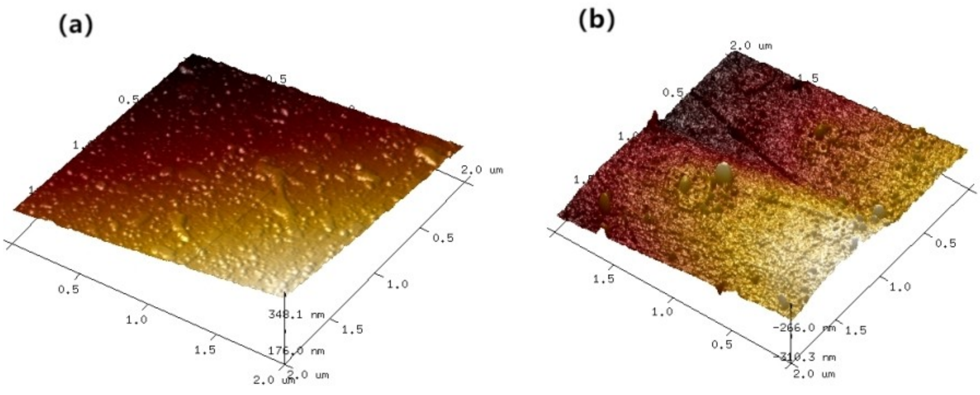

Figure 4. AFM images of (a) the original SPEEK and (b) the S/MWCNT–NH_2–2 PEMs.

Table 1. Physicochemical characteristics of the PEMs.

PEM	Thickness (μm)	IEC (mmol g^{-1})	Proton conductivity (S cm^{-1})	WU% (65 °C)	SR% (65 °C)
Nafion 212	55	0.99	0.267	12.2	10.8
SPEEK 57	56	1.72	0.176	41.5	13.5
S/MWCNT–NH_2–0.7	26	1.84	0.185	43.1	14.2
S/MWCNT–NH_2–1.4	27	1.9	0.194	45.1	15.3
S/MWCNT–NH_2–2	26.5	1.95	0.213	46.5	15.9
S/MWCNT-NH_2–2.5	27	1.92	0.201	45.8	15.6

the AFM images of the original SPEEK PEM and the S/MWCNT–NH_2–2 PEM, and it is obvious that the roughness of the S/MWCNT–NH_2–2 PEM (272 nm) is greater than the original PEM (82.7 nm), which suggests that this hybrid PEM can provide more superficial area for the proton transport and results in a better VE of the battery.[31]

Physicochemical Properties

As shown in Table 1, the IEC, WU, SR, and proton conductivity of the modified PEM was improved with the increase of the MWCNT–NH_2 powder when the content was between 0 wt% and 2 wt%, and decreased when the content was up to 2.5 wt%. This phenomenon is attributed to the strong interactions resulting from the moderate MWCNT–NH_2 and SPEEK polymer matrix, which forms more hydrophilic channels and provides more active sites for proton transport.[32] However, the excessive additions will make the blocking effect of carbon nanotubes dominate, and affect the water absorption of the hybrid PEM.[33] The Cr^{3+}/Fe^{2+} permeability of the hybrid PEM is shown in Figure 5 and Figure S1, and it decreases with the increasing doping degree of MWCNT–NH_2, which is due to the narrow hydrophilic channels that can only allow proton transport while effectively blocking the Cr^{3+}/Fe^{2+} penetration. Besides, the –SO_3^{2-} and –NH_2 groups can form acid-base interactions and reduce the permeability of the Cr^{3+}/Fe^{2+} ions.[34] Ion selectivity depends on the ratio of proton conductivity to Cr^{3+}/Fe^{2+} permeability, which is an essential index for evaluating the comprehensive performance of PEMs. As shown in Figure 5 and Figure S1, when the MWCNT–NH_2 content reaches 2 wt%, the hybrid SPEEK PEM exhibits the highest ion selectivity. For ICRFB, a PEM with good ion selectivity enables great performance of single-cell tests. Therefore, the S/MWCNT–NH_2–2 was used in the following single–cell tests to compare with the original SPEEK and the commercial Nafion 212 PEMs.

The thickness of the SPEEK PEM was adjusted to about 25 μm in our previous work, which resulted in poor mechanical properties. Especially, the lower percentage elongation may cause it to break after hundreds of charge-discharge cycles. As shown in Table 2 and Figure 6, the tensile strength and percentage elongation of the SPEEK PEM are significantly improved with the increase of MWCNT–NH_2 content.[35] Compared with the commercial Nafion 212 PEM which has a bad parameter of tensile strength, the S/MWCNT–NH_2–2 PEM exhibits more balanced mechanical properties.

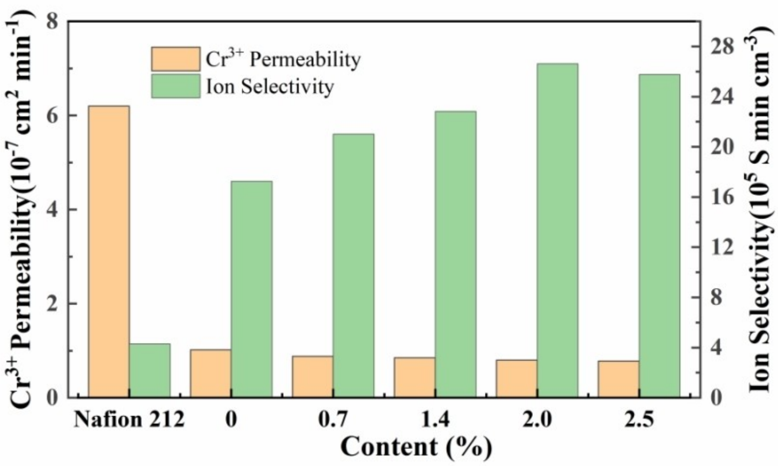

Figure 5. Cr^{3+} permeability and ion selectivity of the SPEEK PEMs modified by different contents of MWCNT–NH_2 and Nafion 212.

Table 2. Mechanical properties of the PEMs.

PEM	Tensile Strength (Mpa)	Percentage Elongation (%)	Young's Modulus (Mpa)
SPEEK 57	24.88	71.15	913.08
S/MWCNT–NH_2–0.7	41.15	94.14	1152.78
S/MWCNT–NH_2–2	44.38	124.8	1192.5
Nafion 212	15.1	187.8	144

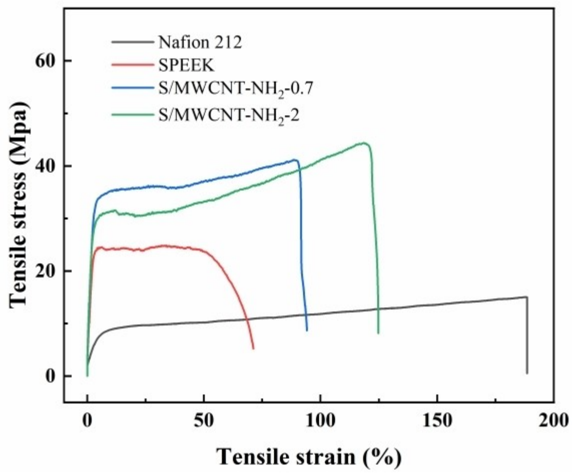

Figure 6. Stress–strain curves of various PEMs.

ICRFB Single–Cells Performance

The optimal doping ratio of S/MWCNT–NH_2–2 for the SPEEK PEM was determined to be 2 wt% by physicochemical properties tests, and this hybrid PEM exhibits the best overall balanced properties of proton conductivity, ionic selectivity, and mechanical properties. In addition, Table 3 intuitively shows that the single–cell containing S/MWCNT–NH_2–2 has the lowest stack resistance compared with the single–cells containing the other SPEEK series PEMs, which is consistent with the results of physicochemical tests.

The efficiencies of the single-cells containing Nafion 212, original SPEEK, and S/MWCNT–NH_2–2 PEMs are shown in Figures 7a–c. It is clear the addition of MWCNT–NH_2–2 resulted in a significant increase in the CE, VE, and EE of the single–cells containing SPEEK series PEMs at each current density, which is in line with the results of the physicochemical properties tests. Notably, the single–cell containing S/MWCNT–NH_2–2 exhibits a higher EE (82.04%) than that of Nafion 212 (81.09%) under 100 mA cm^{-2}, which means the improvement of the SPEEK PEM is successful.[19] During the ICRFB operating process, the cross–contamination of iron ions and chromium ions will result in the phenomenon of self–discharge, and the immensely fast self–discharge will seriously affect the capacity of the battery.[36] Three self–discharge curves are reported in Figure 7d, the ICRFB single–cell containing Nafion 212 only lasted for 6.5 h before the voltage drops, while the single–cell containing the original SPEEK PEM lasted for 14 h. Besides, it is worth noting that the single–cell containing S/MWCNT–NH_2–2 exhibits a 4–hour longer self–discharge time compared with the original SPEEK PEM, which demonstrates that this hybrid PEM has more potential for long–term assemble in the ICRFB in terms of large–scale commercialization.

To further compare the single–cells containing Nafion 212 and S/MWCNT–NH_2–2 PEMs under 100 mA cm^{-2}, the 100 charge–discharge cycles tests were performed. As demonstrated in Figure 8a, in terms of CE, both single–cells are relatively stable while the CE of the single–cell containing S/MWCNT–NH_2–2 obviously exceeds the Nafion 212 throughout the whole process. In terms of EE, although the value of single–cell containing Nafion 212 was very close to the S/MWCNT–NH_2–2 at the beginning, it exhibits a much more rapid degradation tendency during the cycling process. After 100 cycles, the EE of single–cell containing Nafion 212 is lower than the S/MWCNT–NH_2–2 (75.01% and 77.36% respectively), which is due to the single–cell containing Nafion 212 leads to more side reactions[37] during the cycling process, resulting in a serious ohmic polarization and a rapid decrease in voltage efficiency.[38] Figure 8c shows the charge–discharge curves of two single–cells in the first cycle. It can be seen the charge voltage of the single–cell containing Nafion 212 gets higher than that of the S/MWCNT–NH_2–2 as the process goes on, while the discharge voltage gets lower than that of the S/MWCNT–NH_2–2. This is due to the fact that the internal resistance of Nafion 212 is slightly lower than that of the S/MWCNT–NH_2–2 at the beginning, but with the progress of the reaction, the single–cell containing Nafion 212 results in more ion permeation[39,40] and side reactions,[41,42] resulting in a large decrease in its battery capacity, and this phenomenon is more obvious after 100 cycles as shown in Figure 8d. The capacity retention curve in Figure 8b is more intuitively reflecting the excellent capacity retention of the single–cell containing S/MWCNT–NH_2–2 PEM, which means the side reactions and the crossover of the electrolyte of this single–cell are further less than that of the Nafion 212.

The operating temperature of the ICRFB is 65 °C, and the high temperature and strong oxidizing environment will have a great impact on the PEMs in terms of chemical stability and durability. Figure 9 shows the SEM and EDX images of the S/MWCNT–NH_2–2 PEM after all the single–cell tests. It is clear the surface of the PEM remains smooth and complete, and the elements of Cl, Fe, and Cr are uniformly distributed on the

Table 3. The ICRFB stack resistance.

PEM	Nafion 212	SPEEK	S/MWCNT–NH_2–0.7	S/MWCNT–NH_2–1.4	S/MWCNT–NH_2–2	S/MWCNT–NH_2–2.5
Stack resistance (mΩ)	21.03	31.13	28.45	27.21	24.95	26.84

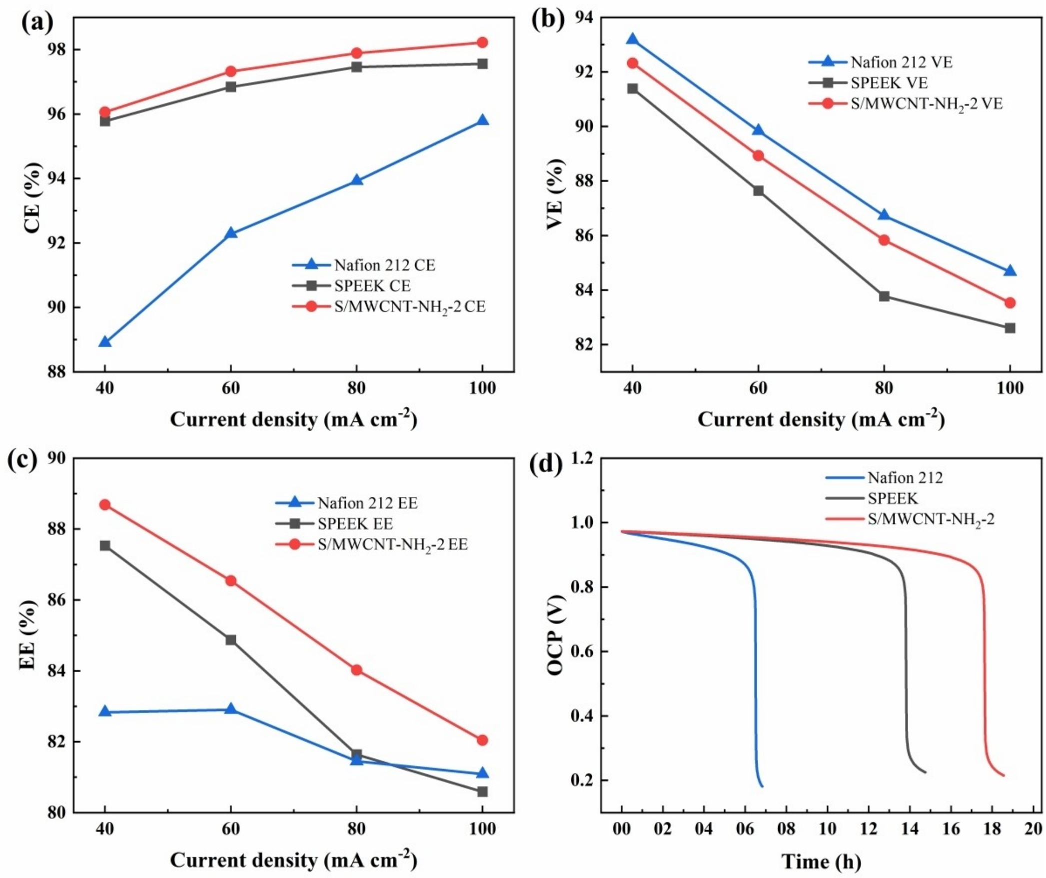

Figure 7. The efficiencies of ICRFB single–cells containing Nafion 212, original SPEEK, and S/MWCNT–NH$_2$–2 PEMs under 40–100 mA cm^{-2}: (a) CE; (b) VE and (c) EE. (d) self–discharge curves (OCP test).

surface of the PEM. The results show that this optimal hybrid PEM has excellent chemical stability to be employed in long-term ICRFB operations.[6]

Capital Cost Analysis

Table 4 shows the materials cost of preparing a 1 m^2 S/MWCNT–NH$_2$–2 PEM. It can be seen that in the case of the complete equipment, the total cost is about 19 \$/m^2, which is much cheaper than Nafion 212 (500 \$/m^2) according to the paper of V. Viswanathan et al.[43] Besides, based on the report of Zeng et al,[44] Figure 10 further depicts that the cost of the membrane as a percentage of a 1 MW–8 h ICRFB energy storage decreases from 39 % to 3 % when Nafion 212 is replaced by S/MWCNT–NH$_2$–2, which result in the estimated cost of an ICRFB system decreases from 194 \$/kWh to 121 \$/kWh.

Table 4. The materials cost of preparing a 1 m^2 S/MWCNT–NH$_2$–2 PEM.

Main materials	Price	Consumption per preparation	Cost per preparation
PEEK	500 g/50 \$	30 g	3 \$
DMF	500 mL/5.6 \$	1000 mL	11.2 \$
MWCNT–NH$_2$	10 g/18 \$	0.6 g	1.08 \$
98 % H_2SO_4	500 mL/5.6 \$	300 mL	3.36 \$
Total			18.64 \$

Conclusions

In this work, the physicochemical characteristics were tested to determine the optimal doping content of the MWCNT–NH$_2$ with SPEEK PEM, and the content was finally determined to be 2 wt %. The S/MWCNT–NH$_2$–2 PEM exhibits the highest ion selectivity and the most balanced mechanical properties, which brings it excellent ICRFB single–cell performance. The single–cell containing S/MWCNT–NH$_2$–2 PEM exhibits higher CE (96.06 %–98.22 %) and EE (82.04 %–88.09 %) under 40–100 mA cm^{-2} than the Nafion 212 (CE: 88.9 %–94.38 %, EE: 81.09 %–82.83 %). Besides, the lower permeability of iron ions and chromium ions through the S/MWCNT–NH$_2$–2 PEM also allows it to have a much longer self-discharge time than the other two PEMs. During the 100 charge–discharge tests, the single-cell containing S/MWCNT–NH$_2$–2 showed a smaller decay range of EE (from 82.67 % to 77.36 %) and less discharge capacity degradation (0.52 % per cycle) than that of the Nafion 212 (EE: from 82.64 % to 75.01 %, discharge capacity degradation: 0.82 % per cycle), which suggests that the S/

Research Article
doi.org/10.1002/batt.202400007

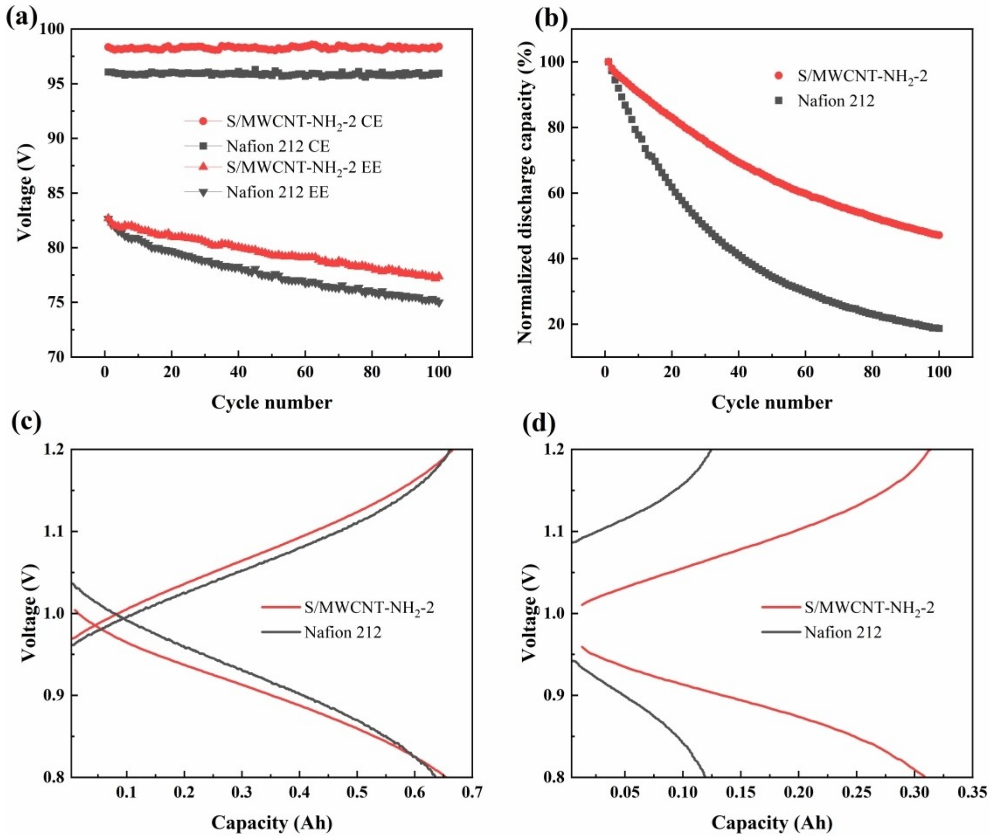

Figure 8. The results of ICRFB single–cells containing Nafion 212, original SPEEK, and S/MWCNT–NH$_2$–2 PEMs in the 100 cycles: (a) CE and EE; (b) discharge capacity retentions; (c) the charge–discharge curves of 1st cycle; (d) the charge–discharge curves of 100th cycle.

MWCNT–NH$_2$–2 with huge advantages of cost and performance has great potential to replace Nafion PEM in the large-scale commercialization of ICRFB. In the next works, we will continue to explore the performance of the hybrid PEM in pilot–scale ICRFB and make further refinements based on the new challenges.

Acknowledgements

This research was funded by the Hubei Polytechnic University Talent Introduction Foundation (No.: 21xjz04R); Key R&D projects of Hubei Provincial Department of Science and Technology (2023DJC187); Open Project of Yantai Research Institute for the Conversion of Old and New Energy (YTDNY20220425-09); the Fundamental Research Projects of Science & Technology Innovation and Development Plan in Yantai City (2022JCYJ043); the Natural Science Foundation of Shandong Province (ZR2022QB068); Youth Talent Introduction

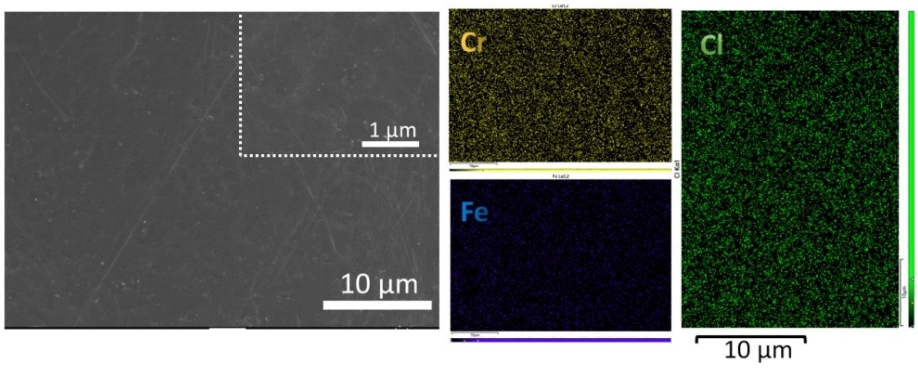

Figure 9. The surface SEM and EDX of the S/MWCNT–NH$_2$–2 PEM after the ICRFB single–cell cycling test.

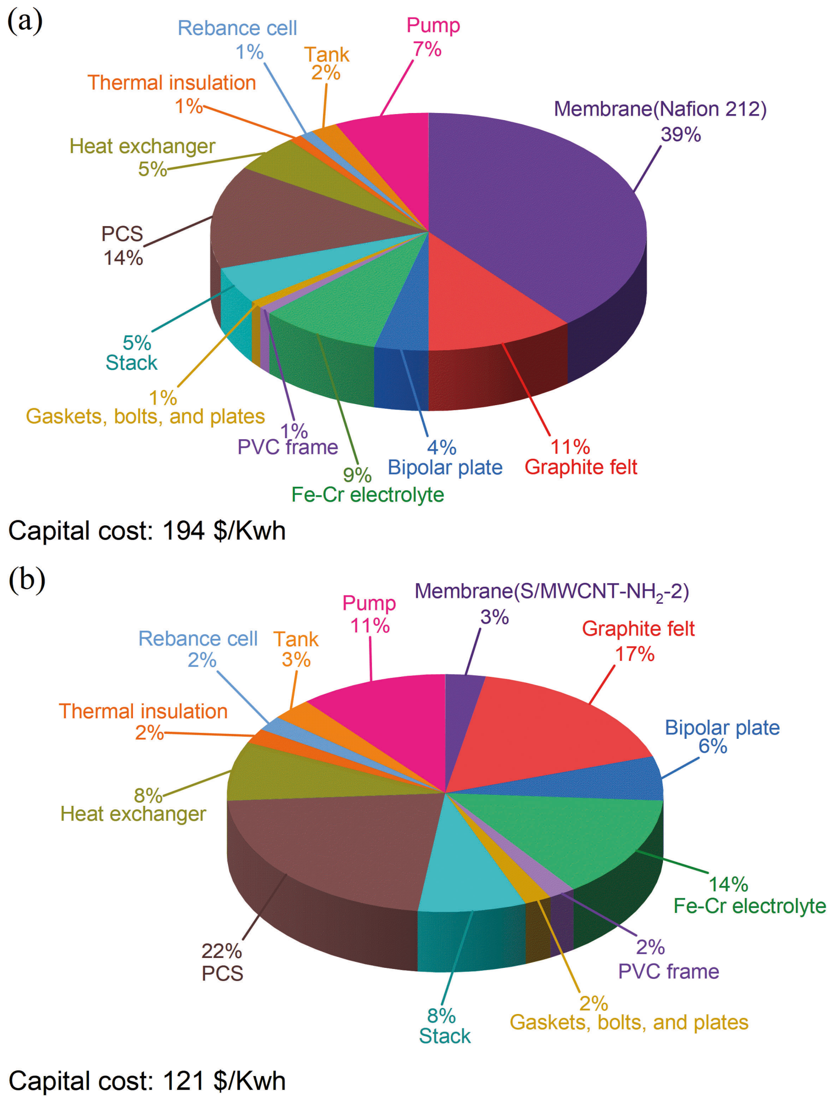

Figure 10. The capital cost of ICRFB containing (a) Nafion 212 and (b) S/MWCNT–NH_2–2 for the 1 MW–8 h energy storage system.

Scientific Research Startup Fee (AUGA2160100623); Heilongjiang Province Talent Introduction Unit Support Funds (AUGA2160501723); National Key R&D Program of China (No.2022YFB4200704). The authors thank Wuhan Chuxin Technology Co., Ltd for providing us with technical and equipment support.

Conflict of Interests

The authors declare no conflict of interest.

Keywords: amino–functionalized multi–walled carbon nanotubes · capacity decay · efficiency · hybrid SPEEK ion exchange membrane · ion selectivity · Iron–chromium redox flow batteries · Nafion physicochemical property · performance · single–cell

[1] C. Sun, H. Zhang, *ChemSusChem* **2022**, *15*, DOI 10.1002/cssc.202101798.
[2] C. T.-C. Wan, K. E. Rodby, M. L. Perry, Y.-M. Chiang, F. R. Brushett, *J. Power Sources* **2023**, *554*, 232248.
[3] A. Pasadakis-Kavounis, F. Arslan, M. Radmer Almind, D. Aili, J. Hjelm, *Batteries & Supercaps* **2023**, *6*, e202300176.
[4] Y. K. Zeng, T. S. Zhao, X. L. Zhou, L. Wei, H. R. Jiang, *J. Power Sources* **2016**, *330*, 55–60.
[5] C. Minke, T. Turek, *J. Power Sources* **2015**, *286*, 247–257.
[6] J. Xi, Z. Li, L. Yu, B. Yin, L. Wang, L. Liu, X. Qiu, L. Chen, *J. Power Sources* **2015**, *285*, 195–204.
[7] C.-Y. Sun, H. Zhang, X.-D. Luo, N. Chen, *Ionics* **2019**, *25*, 4219–4229.
[8] G. Wang, F. Wang, A. Li, M. Zhang, J. Zhang, J. Chen, R. Wang, *J. Appl. Polym. Sci.* **2020**, *137*, 48830.
[9] J. Ye, X. Zhao, Y. Ma, J. Su, C. Xiang, K. Zhao, M. Ding, C. Jia, L. Sun, *Adv. Energy Mater.* **2020**, *10*, 1904041.
[10] C. Sun, E. Negro, A. Nale, G. Pagot, K. Vezzù, T. A. Zawodzinski, L. Meda, C. Gambaro, V. Di Noto, *Electrochim. Acta* **2021**, *378*, 138133.
[11] X. Lou, H. Fu, J. Xu, Y. Long, S. Yan, H. Zou, B. Lu, M. He, M. Ding, X. Zhu, C. Jia, *Energy Mater. Adv.* **2022**, *2022*, 9865618.
[12] X. Lou, B. Lu, M. He, Y. Yu, X. Zhu, F. Peng, C. Qin, M. Ding, C. Jia, *J. Membr. Sci.* **2022**, *643*, 120015.
[13] S. Sophia, E. Abouzari Lotf, A. Ahmad, P. Moozarm Nia, R. Rasit Ali, *E3S Web Conf.* **2019**, *90*, 01004.
[14] X. Lou, D. Yuan, Y. Yu, Y. Lei, M. Ding, Q. Sun, C. Jia, *Chem. Asian J.* **2020**, *15*, 2357–2363.

[15] M. He, M. Guan, R. Zhan, K. Zhou, H. Fu, X. Wang, F. Zhong, M. Ding, C. Jia, *Chem. Asian J.* **2023**, *18*, e202201152.
[16] J. Ye, Y. Cheng, L. Sun, M. Ding, C. Wu, D. Yuan, X. Zhao, C. Xiang, C. Jia, *J. Membr. Sci.* **2019**, *572*, 110–118.
[17] J. Ye, D. Yuan, M. Ding, Y. Long, T. Long, L. Sun, C. Jia, *J. Power Sources* **2021**, *482*, 229023.
[18] S. Jiang, H. Wang, L. Li, C. Zhao, J. Sheng, H. Shi, *J. Membr. Sci.* **2023**, *671*, 121394.
[19] E. Bai, H. Zhu, C. Sun, G. Liu, X. Xie, C. Xu, S. Wu, *Membranes* **2023**, *13*, 820.
[20] J. Xu, R. D. Deshpande, J. Pan, Y.-T. Cheng, V. S. Battaglia, *J. Electrochem. Soc.* **2015**, *162*, A2026–A2035.
[21] J. Li, Q. Zhang, S. Peng, D. Zhang, X. Yan, X. Wu, X. Gong, Q. Wang, G. He, *J. Membr. Sci.* **2019**, *583*, 93–102.
[22] Y. Quan, G. Wang, A. Li, X. Wei, F. Li, J. Zhang, J. Chen, R. Wang, *RSC Adv.* **2019**, *9*, 3838–3846.
[23] C. Sun, E. Negro, K. Vezzù, G. Pagot, G. Cavinato, A. Nale, Y. Herve Bang, V. Di Noto, *Electrochim. Acta* **2019**, *309*, 311–325.
[24] L. G. da Trindade, L. Zanchet, R. Dreon, J. C. Souza, M. Assis, E. Longo, E. M. A. Martini, A. J. Chiquito, F. M. Pontes, *J. Mater. Sci.* **2020**, *55*, 14938–14952.
[25] S. Wang, Z. Xu, X. Wu, H. Zhao, J. Zhao, J. Liu, C. Yan, X. Fan, *Appl. Energy* **2020**, *271*, 115252.
[26] S. Wang, Z. Xu, X. Wu, H. Zhao, J. Zhao, J. Liu, C. Yan, X. Fan, *Electrochim. Acta* **2021**, *368*, 137524.
[27] C. Sun, H. Zhang, *Int. J. Energy Res.* **2019**, er.4875.
[28] H. Zhu, E. Bai, C. Sun, G. Liu, Z. Zhang, X. Xie, C. Xu, S. Wu, *J. Mater. Sci.* **2023**, *58*, 17313–17325.
[29] X. Li, H. Zhang, Z. Mai, H. Zhang, I. Vankelecom, *Energy Environ. Sci.* **2011**, *4*, 1147–1160.
[30] D. Vidhyeswari, A. Surendhar, S. Bhuvaneshwari, *Chemosphere* **2022**, *293*, 133560.
[31] C. Jia, Y. Cheng, X. Ling, G. Wei, J. Liu, C. Yan, *Electrochim. Acta* **2015**, *153*, 44–48.
[32] M. Ding, X. Ling, D. Yuan, Y. Cheng, C. Wu, Z.-S. Chao, L. Sun, C. Yan, C. Jia, *Front. Chem.* **2018**, *6*, 286.
[33] C. Tseng, Y. Ye, M. Cheng, K. Kao, W. Shen, J. Rick, J. Chen, B. Hwang, *Adv. Energy Mater.* **2011**, *1*, 1220–1224.
[34] R. Niu, L. Kong, L. Zheng, H. Wang, H. Shi, *J. Membr. Sci.* **2017**, *525*, 220–228.
[35] S. Gahlot, P. P. Sharma, P. K. Jha, V. Kulshrestha, *Macromol. Symp.* **2017**, *376*, 1700048.
[36] J. Sun, D. Shi, H. Zhong, X. Li, H. Zhang, *J. Power Sources* **2015**, *294*, 562–568.
[37] S. Zhang, W. Guo, F. Yang, P. Zheng, R. Qiao, Z. Li, *Batteries & Supercaps* **2019**, *2*, 627–637.
[38] H. Zhang, Y. Tan, X. Luo, C. Sun, N. Chen, *ChemElectroChem* **2019**, *6*, 3175–3188.
[39] R. P. Naresh, K. Mariyappan, D. Dixon, M. Ulaganathan, P. Ragupathy, *Batteries & Supercaps* **2021**, *4*, 1464–1472.
[40] T. Haisch, H. Ji, L. Holtz, T. Struckmann, C. Weidlich, *Membranes* **2021**, *11*, 232.
[41] A. Tang, J. Bao, M. Skyllas-Kazacos, *J. Power Sources* **2011**, *196*, 10737–10747.
[42] Y. K. Zeng, T. S. Zhao, X. L. Zhou, J. Zou, Y. X. Ren, *J. Power Sources* **2017**, *352*, 77–82.
[43] V. Viswanathan, A. Crawford, D. Stephenson, S. Kim, W. Wang, B. Li, G. Coffey, E. Thomsen, G. Graff, P. Balducci, M. Kintner-Meyer, V. Sprenkle, *J. Power Sources* **2014**, *247*, 1040–1051.
[44] Y. K. Zeng, T. S. Zhao, L. An, X. L. Zhou, L. Wei, *J. Power Sources* **2015**, *300*, 438–443.

Manuscript received: January 11, 2024
Revised manuscript received: March 11, 2024
Accepted manuscript online: March 17, 2024
Version of record online: April 30, 2024